Colloids and Surfaces B: Biointerfaces 135 (2015) 833–839

Contents lists available at ScienceDirect

Colloids and Surfaces B: Biointerfaces

journal homepage: www.elsevier.com/locate/colsurfb

Nanostructured sensor based on carbon nanotubes and clavanin A for bacterial detection

César A.S. Andrade[a,b,*], Jéssica M. Nascimento[a], Idjane S. Oliveira[c], Carlos V.J. de Oliveira[b], Celso P. de Melo[d], Octávio L. Franco[e,f], Maria D.L. Oliveira[b]

[a] Programa de Pós-Graduação em Inovação Terapêutica, Universidade Federal de Pernambuco, 50670-901 Recife, PE, Brazil
[b] Departamento de Bioquímica, Universidade Federal de Pernambuco, 50670-901 Recife, PE, Brazil
[c] Centro Acadêmico de Vitória, Universidade Federal de Pernambuco, 55608-680 Vitória de Santo Antão, PE, Brazil
[d] Departamento de Física, Universidade Federal de Pernambuco, 50670-901 Recife, PE, Brazil
[e] Centro de Análise Proteômicas e Bioquímicas de Brasília, Universidade Católica de Brasília, Brasília, DF, Brazil
[f] S-Inova, Pós-graduação em Biotecnologia, Universidade Católica Dom Bosco, Campo Grande, MS, Brazil

ARTICLE INFO

Article history:
Received 22 December 2014
Received in revised form 11 March 2015
Accepted 16 March 2015
Available online 24 March 2015

Keywords:
Biosensor
Carbon nanotubes
Bacteria
Antimicrobial peptides
Electrochemical impedance spectroscopy

ABSTRACT

Unusual methods for specific detection of pathogenic bacteria are becoming key points for control and identification of problems related to health and (bio)safety. In this context, this work aims to propose a new approach for the development of nanostructured biosensors based on carbon nanotubes (CNTs) and antimicrobial peptides for bacterial detection. Firstly, the antimicrobial peptide clavanin A (ClavA) was chemically immobilized on CNTs and surface-immobilized ClavA was used to detect *Klebsiella pneumoniae*, *Enterococcus faecalis*, *Escherichia coli* and *Bacillus subtilis* in a direct assay format. We used electrochemical impedance spectroscopy technique to evaluate the effectiveness and sensitivity of the ClavA-based biosensors by measuring the modifications in their electrochemical responses before and after incubation in presence of different bacteria concentrations. The biosensor was able to discriminate between bacteria concentrations in the 10^2–10^6 CFU mL^{-1} range. Atomic force microscopy analysis confirmed the biosensor functionality for bacterial recognition. This new sensor system was capable of differentiating between Gram-positive and Gram-negative bacteria, since ClavA showed different affinities toward the pathogenic bacteria species.

1. Introduction

Nowadays, due to increasing levels of bacterial resistance infectious diseases are once again being considered as a severe worldwide health problem. In that regard, *Klebsiella pneumoniae* is an opportunistic pathogen associated at different cases of infections across the world. *K. pneumoniae* has been recognized in the group of "ESKAPE" pathogens (*Enterococcus faecium*, *Staphylococcus aureus*, *Klebsiella pneumoniae*, *Acinetobacter baumannii*, *Pseudomonas aeruginosa*, and *Enterobacter* species), which present high resistance to conventional antibiotics [1]. Also, *Escherichia coli*, a notorious cause of food poisoning Gram-negative bacterium, produces toxins that may cause multiple symptoms including skin irritation, vomiting, nausea, diarrhea, fever, inflammations, and liver damage [2]. Hence, the diagnosis and control of microbial diseases are a problem of increasing importance in public health. The most common methods for detection and quantification of bacteria are based on separation techniques, culture and colony counting, molecular tests, and on biochemical and immunologic assays [3]. The classical methods have some clear disadvantages, as the cost of the necessary equipment and the long periods required of analysis. Although diverse alternative methods for fast bacteria detection have been developed, some of them require pretreatment to extract DNA from the target samples, as polymerase chain reaction (PCR) [4], DNA-based nanobarcode [5] and MALDI MS analyses [6]. Unfortunately, the use of these more technological methods in high-throughput pathogen detection requires the presence of properly trained staff with access to expensive devices [7]. Therefore, the development of new methods of detecting microorganisms that dispense pre-treatment, while providing a fast detection, selectivity and sensitivity, continues to be extremely desirable.

Due to their outstanding selectivity, antimicrobial peptides (AMPs) are suitable candidates for the development of future antibiotics [8]. The ability of the AMPs to interact with microorganisms is mainly due to their ability to target the outer membrane

* Corresponding author at: Departamento de Bioquímica, UFPE, 50670-901 Recife, PE, Brazil. Tel.: +55 81 2126 8450; fax: +55 81 2126 8547.
E-mail address: csrandrade@gmail.com (C.A.S. Andrade).

http://dx.doi.org/10.1016/j.colsurfb.2015.03.037
0927-7765/

of bacterial cells, leading to a disruption of electrochemical gradient across the cell, causing the final rupture of the cellular membrane-cell integrity [9]. It is important to note that the membrane selectivity varies for different peptides [10], with a distinct specificity of interaction between eukaryotic or prokaryotic cell membranes [11]. Among such peptides are the clavanins, previously isolated from hemocytes from the invertebrate *Styela clava*, a solitary tunicate [12]. Clavanin A (Clav A) is a helical peptide with a 23-amino-acid residues length [13]. Moreover, Clav A is well known to be highly effective against Gram-positive and Gram-negative organisms [14].

It is worth to note that the development of AMPs based biosensors for the detection of pathogenic bacteria could impact areas as diverse as water-quality monitoring, testing of pharmaceutical products and analyses of bacterial contamination [15]. Some authors have used AMPs as bio recognition elements for the development of microorganism biosensors with detection limits of 5×10^4 cells mL^{-1} [16,17].

Meanwhile, many researchers have focused efforts in the study of carbon nanotubes (CNTs) due to their remarkable sensitivity to structural changes, large length-to-diameter aspect ratios that provide high surface-to-volume ratios and the possibility of simple chemical modifications [18]. CNTs may be assembled in single-walled (SWCNTs) or multi-walled (MWCNTs) nanotubes. SWCNTs have typically 1 nm of diameter while MWCNTs tend to have diameters between 2 and 100 nm [19]. As a general trend, CNTs have shown suitable properties for electrochemical biosensing due to their ability to accumulate analytes, minimal surface fouling and good electrocatalytic activity [20,21].

Electrochemical Impedance Spectroscopy (EIS) is an electroanalytical technique that measures the impedance, a complex parameter that comprises capacitance and resistance, after the application of small amplitude sinusoidal voltage signal to the sample of interest placed on an electrochemical cell, resulting in a measurable current response [22]. This technique can then be conveniently applied to the analysis of (bio)electrochemical processes that occur at the electrode/solution interface [23]. It is worthy to note that electrochemical approach is cost-effective, not requiring expensive instrumentation [24] and allowing a good limit of the portability [25].

The aim of the present paper is to describe the development of a selective and sensitive sensor for monitoring Gram-positive and Gram-negative bacteria based on COOH-functionalized carbon nanotubes and ClavA using EIS. COOH-functionalized MWCNTs are known to be excellent analytical platforms to immobilize peptides. The infectious agents tested were *E. coli* ATCC 25222, *K. pneumoniae* ATCC 29665, *Enterococcus faecalis* ATCC 29212 and *Bacillus subtilis* ATCC 6633, a non-infectious bacterium used as a control system.

2. Experimental

2.1. Materials

Multi-walled carbon nanotubes (>8% carboxylic acid functionalized, avg. diam. of 9.5 nm and length of 1.5 μm), cysteine, 1-ethyl-3-(3-dimethylaminopropyl) carbodiimide (EDC) and N-hydroxysuccinimide (NHS) were purchased from Sigma–Aldrich (St. Louis, USA). Potassium ferri- and ferrocyanide were obtained from VETEC (Brazil). The bacteria strains were cultured in according to standard microbiological methods, using adequately sterilized materials, solutions and culturing nutrient agar medium. All chemicals and solvents were of analytical grade and have been used as received, without further purification. All water used in the experiments was obtained from a Milli-Q plus (Billerica, USA) purification system.

2.2. Peptide synthesis

Clavanin A was synthesized by Peptides 2.0 (USA) using the solid-phase with the N-9-fluorenylmethyloxycarbonyl (Fmoc) strategy and purified by high-performance liquid chromatography (HPLC). Peptide purity used in biologic assays was higher than 95%. Moreover, sequence and purity degree was confirmed by MALDI-ToF analyses (data not shown).

2.3. Microorganism culturing

All bacteria strains were cultivated under the same experimental conditions, including incubation time and temperature. The bacteria were immobilized using the adapted protocol described in Vazquez et al. [26]. The bacteria were grown in Brain Heart Infusion medium for 24 h at 37 °C. Then, for each one of the species considered, we prepared concentrated bacterial suspension with 10 mL of sterile PBS, resulting in a concentration of approximately 15×10^8 CFU mL^{-1}, compatible with the turbidity, which was evaluated as tube 5 in the McFarland scale. The bacterial suspension was centrifuged for 10 min at 3000 rpm; after the supernatant was discarded, the pellet was washed three times with sterile PBS (pH 7.4). Then, we used formalin solution 0.4 in sterile water for 2 h to 4 °C, shaking the tube by inversion, to immobilize the bacteria. After incubation in 2 h formaldehyde, the bacteria were washed with PBS solution sterile for three times. Finally, the turbidity of the bacterial suspension was adjusted tube 5 in the McFarland scale and stored at 4 °C until use.

2.4. Biosensor preparation and bacteria detection

The surface of the bare gold electrode was carefully polished using 25 μm grain size polishing alumina. The pretreated electrode was immersed in cysteine aqueous solution for 10 min to obtain a self-assembled monolayer. Thereafter, the cys-modified electrode was treated with 0.4 M EDC-0.1 M NHS for 10 min to convert the terminal carboxylic group to activate the NHS ester [27]. Subsequently, 1 μL of CNTs was dropped on the EDC:NHS-Cys-modified electrode and the procedure for activate the NHS ester was repeated. Finally, the EDC:NHS-CNTs-EDC:NHS-Cys-modified electrode was immersed in a solution of ClavA (1 mg mL^{-1}). 1 μL of each solution containing different concentrations of the bacterial cells were dropped on the ClavA-CNTs-Cys-modified electrode and waiting for 10 min. To remove the nonspecifically bound molecules, the sensor was washed with phosphate buffer saline (PBS, pH 7.4).

2.5. Electrochemical measurements

We carried out EIS measurements using a Autolab PGSTAT 128N potentiostat/galvanostat (Ecochemie, The Netherlands) controlled by NOVA 1.8 software. We used a 10 mM $K_4[Fe(CN)_6]/K_3[Fe(CN)_6]$ (1:1) solution in all experiments as a redox probe in PBS (pH 7.4). The electrochemical experiments were performed in a conventional electrochemical cell containing three electrodes, using Ag/AgCl (3 M in KCl) as reference, platinum as counter electrode and a bare gold electrode ($\phi = 2$ mm) as working electrode. Nyquist plots were obtained in a frequency range varying between 100 mHz and 100 kHz with a 10 mV amplitude of the applied sine wave potential. All electrochemical measurements were performed at room temperature and inside a Faraday cage. Three different samples of each bacterium ($n = 3$) were run in triplicate for all measurements.

2.6. Atomic force microscopy measurements

Morphological analysis was performed using a commercial PicoSPM II atomic force microscopy (AFM) (Molecular Imaging,

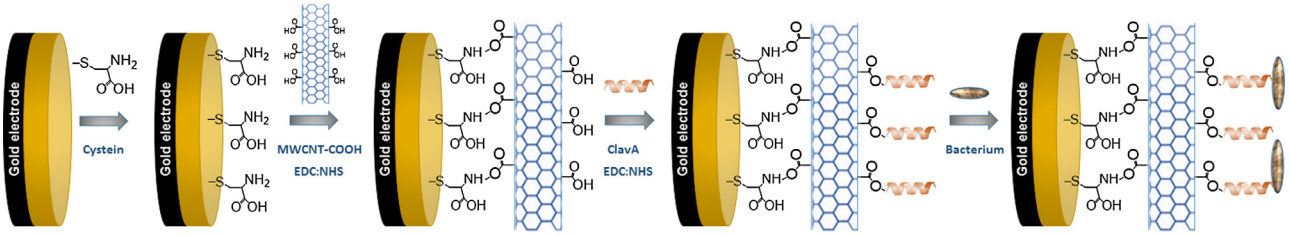

Fig. 1. Schematic representation of the fabrication process of the biosensor.

USA) by means of non-contact mode AFM in air at room temperature (approximately 25 °C). The images were obtained using cantilevers with a silicon tip with a resonance frequency of 297 kHz (Nanosensors, Switzerland).

3. Results and discussion

3.1. Preparation and morphological analysis of the sensor system

The aim of this study was the development of a sensor for detection of a broad variety of microbial species. We present a schematic diagram of the sensor system in Fig. 1. Initially, a Cys self-assembled monolayer is formed on the bare gold electrode surface. After that, the surface was activated by the formation of NHS ester using EDC:NHS solution [27], allowing the coupling of the CNTs. Finally, the peptide is bound on the CNTs surface and the interaction of the sensor with the bacteria is evaluated. The immobilization of ClavA on the CNTs was carried out through a stable acyl amino ester intermediate that was generated by the EDC:NHS solution.

In Fig. 2 we show typical AFM topographical images of the stepwise processes adopted in the manufacturing of the biosensor and in the testing against bacteria. In Fig. 2a one can see a densely packed self-assembled Cys monolayer, in an evidence of a homogeneous uniform covering of the gold electrode surface, with a mean height of (17.1 ± 2.3) nm, in agreement to a previous work [28]. The height of the CNTs covalently linked on the Cys monolayer corresponds to (10.2 ± 3.1) nm and appears to be constant over its entire length (Fig. 2b). Subsequently, COOH functional groups on CNTs surfaces were modified with ClavA, resulting in an apparent increment of height of about 2–4 nm (Fig. 2c). According to Zorbas et al. [29], when peptides become attached to the carbon nanotubes an additional height of 1–3 nm results.

We observed a significant increase in the roughness of the sensor surface after the interaction with the bacteria occurs. In addition, the observed differences in the film roughness could be correlated to the specificity of ClavA for diverse bacteria. The typical heights of the different bacteria *E. coli*, *K. pneumoniae*, *E. faecalis* and *B. subtilis* on the sensor surface were (384.6 ± 28.5) nm, (379.5 ± 31.9) nm,

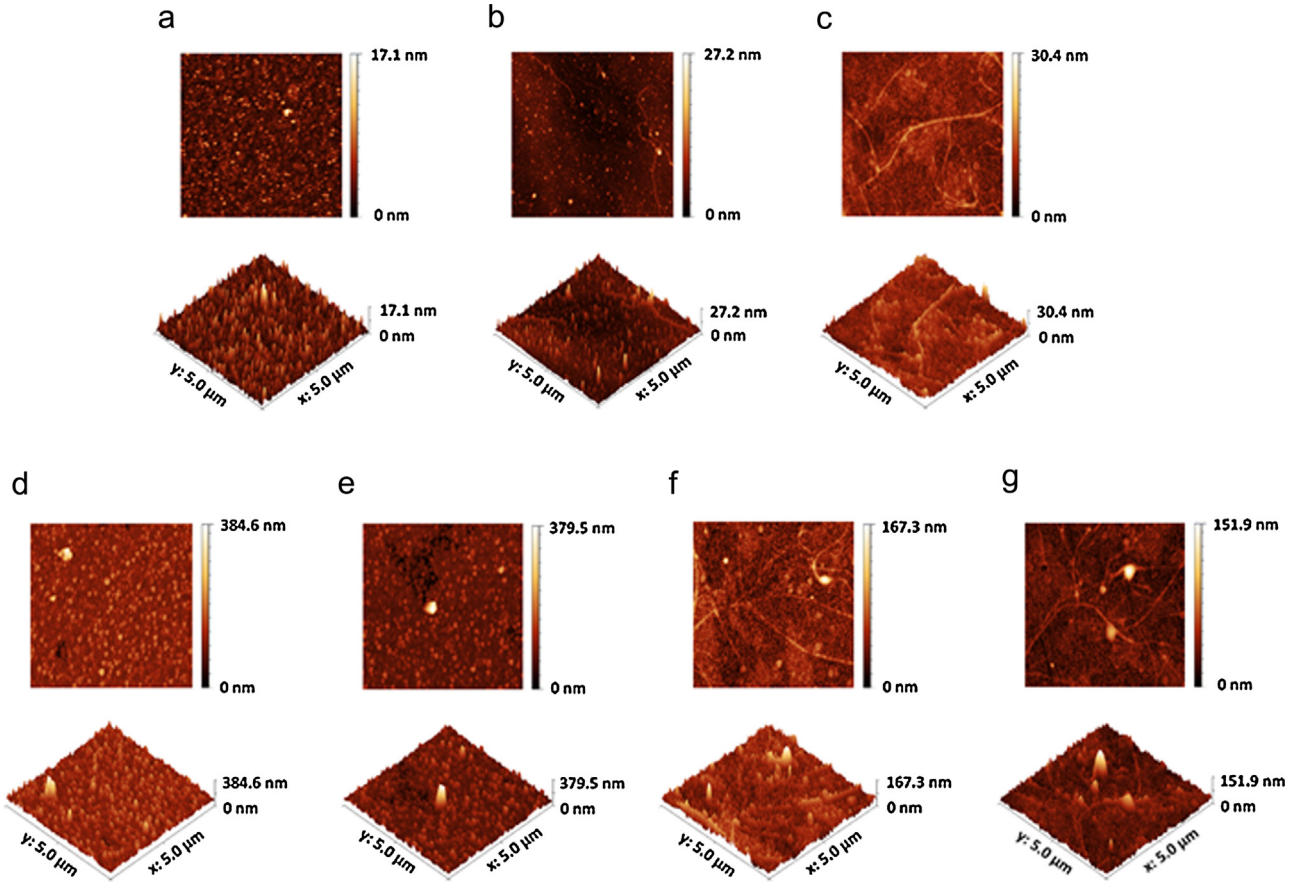

Fig. 2. AFM images of the gold electrode coated with Cys (a), Cys-CNTs (b), Cys-CNTs-ClavA(c), Cys-CNTs-ClavA-*E. coli* (d), Cys-CNTs-ClavA-*K. pneumoniae* (e), Cys-CNTs-ClavA-*E. faecalis* (f) and Cys-CNTs-ClavA-*B. subtilis* (g).

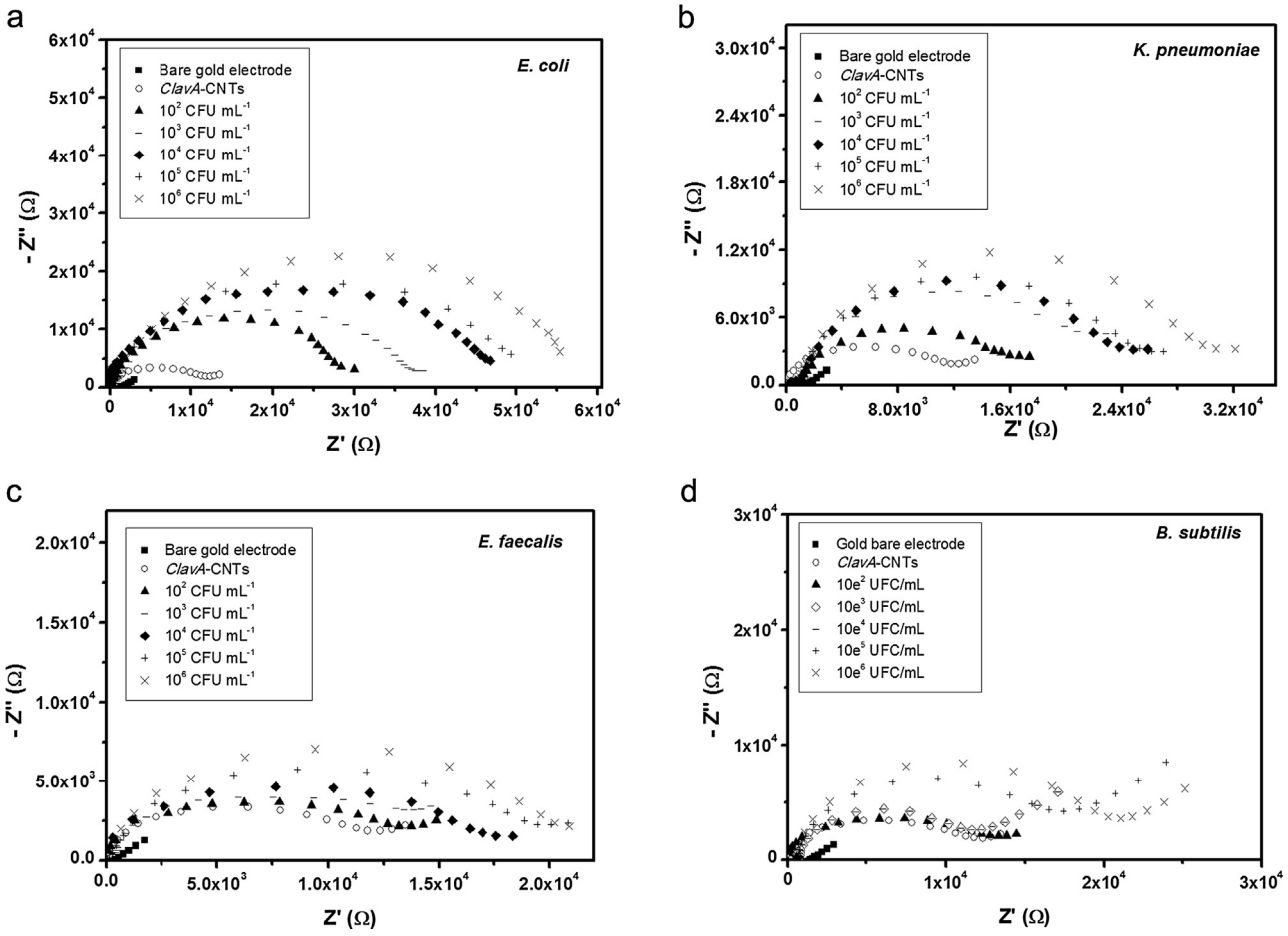

Fig. 3. Nyquist plots of the stepwise immobilization of Cys-CNTs-ClavA and peptide interaction with different bacteria (a) *E. coli*, (b) *K. pneumoniae*, (c) *E. faecalis* and (d) *B. subtilis*. The impedance spectra were taken for 10 mM $[Fe(CN)_6]^{4-}$/$[Fe(CN)_6]^{3-}$ 1:1 + 0.15 M NaCl in 10 mM PBS (pH 7.4) in the frequency range from 100 mHz to 100 kHz. All electrochemical measurements were performed in triplicate using three different samples ($n = 3$).

(167.3 ± 26.3) nm and (151.9 ± 24.6) nm, respectively (Fig. 2d–g). In Fig. 2d we show that a complete covering of the sensor surface occurs due to the sensor recognition of *E. coli* bacteria. *K. pneumoniae* bacterium, otherwise, does not appear to be continuously attached across the biosensor surface (Fig. 2e). Also, as shown in Fig. 2f and g, the sensor system has a non-significant recognition for *E. faecalis* and *B. subtilis* bacteria.

3.2. Selectivity of the sensor

EIS is a powerful technique that has shown high sensitivity and specificity when applied to the study of biosensor interfaces [30]. One should stress that selectivity in bacteria detection is an important factor for biosensors development. Since our studies were aimed to the elucidation of factors determining the selectivity of the sensor for pathogenic Gram-negative vs. Gram-positive species, by using a non-pathogenic species as control, we investigated the selectivity of our sensor system toward diverse bacterial species, including *E. coli*, *K. pneumoniae*, *E. faecalis* and non-pathogenic *B. subtilis*.

It is important to describe that sensor selectivity will be directly related to AMP specificity. In our case clavanin A is a promiscuous peptide with ability to control both Gram-positive and -negative bacteria [31], a fact that should reduce the possibility of better discriminating between them. Moreover, this low selectivity seems to be intrinsic related to the nature of AMPs, which are small amphiphilic compounds with ability to bind to multiple targets at same time [32]. Mannoor et al. [15] demonstrated that AMP is a useful molecule for the development of biosensors for microorganisms, since a dramatic change in the dielectric properties of the system seems to occur when the sensor is in contact with the bacteria. According to Zelada-Guillen et al. [33], the detection of microorganisms in liquid samples based on electric measurements requires control of the ionic strength of the sample, due to the presence of different charged species in the samples that may induce false-positive responses. Because of that, the microorganisms used in this work were further eluted in a controlled PBS medium, prior to impedimetric measurement with the biosensor.

The Nyquist impedance plots of the stepwise process are shown in Fig. 3. Nyquist plots show the simultaneous changes in the real (Z′) and imaginary (Z″) parts of the complex impedance over the entire frequency range. ClavA immobilized in ClavA-CNTs-Cys-modified electrode exhibited a clear distinction of binding toward Gram-negative and Gram-positive species (Fig. 3a–d). The sensor obtained had a higher selectivity for Gram-negative bacteria than toward Gram-positive bacteria and non-pathogenic *B. subtilis*; for instance, ClavA exhibited a higher impedimetric response for Gram-negative species (*E. coli* and *K. pneumoniae*) than to Gram-positive species (*E. faecalis* and *B. subtilis*). Indeed, other authors [14,15,34] have previously demonstrated the ability of antimicrobial peptides to selectively differentiate between Gram-negative and Gram-positive bacteria.

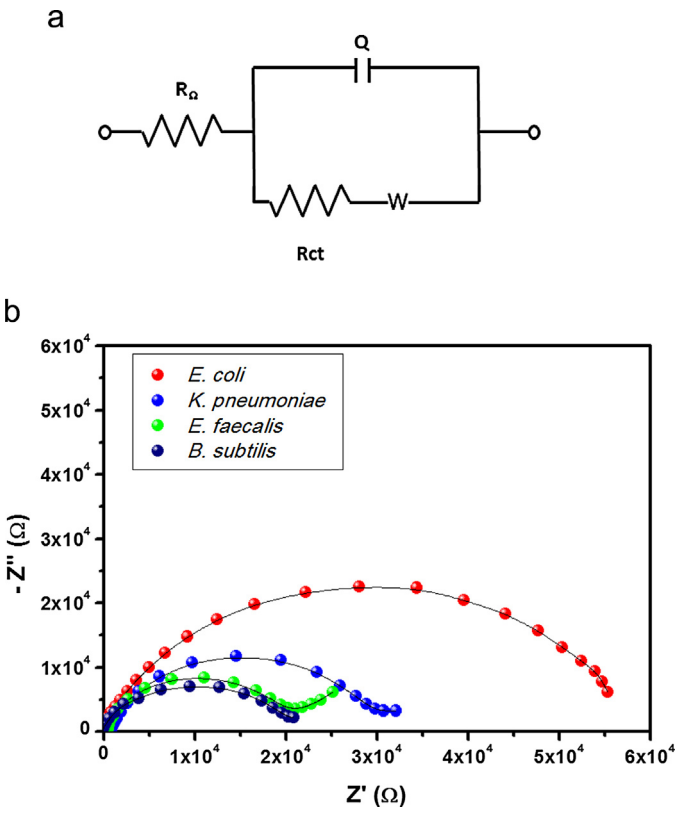

Fig. 4. Equivalent circuit (a) adopted to fit the impedance data where R_Ω is the ohmic resistance of the electrolyte solution, Q the phase constant element, Z_W the Warburg impedance, and R_{CT} the electron-transfer resistance and (b) Nyquist plots of the sensor system and its respective interaction with genomic DNA target at different concentrations. Supporting electrolyte: 10 mM $[Fe(CN)_6]^{4-}/[Fe(CN)_6]^{3-}$ 1:1 + 0.15 M NaCl in 10 mM PBS (pH 7.4) solution; scan rate of 50 mV s^{-1}.

The selectivity of peptides for Gram-positive and Gram-negative bacteria can be explained by the balance that must exist between electrostatic and hydrophobic interactions, a phenomenon that could underlie the mechanism of bacterial cell binding by AMPs [8,15]. Gram-negative and Gram-positive bacteria have differences in their membrane structures, which contributes for their characteristic responses in presence of the peptide. Of note, negatively charged lipopolysaccharides (LPS) are found in the outer membrane of Gram-negative bacteria, as well as a thin peptidoglycan layer. On the other hand, Gram-positive bacteria are composed by a thick peptidoglycan layer and a cell wall composed by teichoics and lipoteichoics acid.

As shown in Fig. 3a–d, the ClavA-CNTs-Cys-modified electrode was able to differentiate between Gram-positive and Gram-negative bacteria. From the analyses of the Nyquist plot at low frequencies, it was observed that the measured value of real part of the impedance increases with the increase in the concentration of the microorganism cells present in the samples. It is important to note that this response is proportional to the number of bacterium cells, with the higher response being observed for 10^6 CFU mL^{-1}. In addition, the contribution from the microorganism cells to the impedance response of the system begins to be noticeable with a decrease in frequency, as a result of the increasing dielectric relaxation of the smaller dipoles (including those of water molecules) in the buffer solution, upon [15].

In Fig. 4a we show the equivalent model circuit that gives an electrical response equivalent to that of the Nyquist plot of interest. This equivalent circuit is composed by a solution resistance (R_s) in series with a phase constant element (Q) and charge transfer resistance (R_{ct}) disposed in parallel. While R_{ct} and Q depend on the dielectric and insulating features at the electrode/electrolyte interface, R_{ct} is directly related to the kinetics of the redox reaction. On the other hand, Q is related to the heterogeneous nature of the electrode/solution interface as, for instance, the dispersion caused by the surface roughness [35]. In addition, the capacitance of the modified electrode is inversely proportional to the thickness of the dielectric layer [36]. The changes in the R_{ct} during the deposition of molecules on the sensor surface can be measured in presence of a redox mediator, a process known as Faradic impedance. At intermediate frequencies, the Nyquist diagram consists in a semicircle segment that corresponds to the electron-transfer limited process. Finally, at low frequencies a straight-line segment that represents diffusion limited electron transfer process is observed.

Our results demonstrate that the peptide retains the capability to act at the bacterial membrane surface (Table 1). As it can be seen from the data represented in Fig. 4b, an increase in the charge transfer resistance (R_{ct}) follows the increase of the bacterial concentration; hence, the performance of the modified electrode for detection of bacteria may be evaluated through the relative variation of this parameter (ΔR_{ct}) [30], according to

$$\Delta R_{CT}(\%) = \frac{R_{CT(recog)} - R_{CT(sensor)}}{R_{CT(sensor)}} \times 100, \quad (1)$$

where $R_{CT(recog)}$ is the value of the electron-transfer resistance after the bacterial peptide recognition, and $R_{CT(sensor)}$ corresponds to the R_{CT} value of the sensor layer. The ΔR_{CT} results can be used to assess the sensitivity for the presence of pathogenic and non-pathogenic bacteria. In the cases of *E. coli* and *K. pneumoniae* (Fig. 5), we have found a trend for saturation in the relationship between the ΔR_{CT} and bacteria CFU mL^{-1}, indicating that the interactions between ClavA and these bacterial cells can be sensed by the modified electrode. We found lower values of ΔR_{CT} in the cases of *E. faecalis* and *B. subtilis*, a fact that reflects the ClavA capability in interacting with surface structures present in Gram-negative pathogenic strains. A detection limit of 10^2 CFU mL^{-1} was estimated from the signal-to-noise (S/N) characteristics of these data ($S/N \cong 3$), where the S/N ratio was obtained by taking the quotient of the impedimetric variation to the standard deviation [37]. We also evaluated unspecific interactions in the sensor system by exposing a SWCNT electrode not functionalized with the ClavA to increasing concentrations of bacteria, starting from 10^2 CFU mL^{-1} up to 10^6 CFU mL^{-1}; the fact that no response was obtained confirms the importance of ClavA functionalization of the carbon nanotubes.

In general, the interaction between AMPs and bacteria increases the R_{ct} due to the blocking of the electron transfer between redox pair and electrode surface. Therefore, occurs a reduction of the effective area associated to the increase of the R_{ct} and consequently a decrease in the phase constant element (Q) [38]. It should be noted, however, that the exact reasons why non-specific binding occurs is not completely elucidate [38].

The low detection limits achieved demonstrate that our sensor system could be used to detect bacteria in complex samples at concentrations close to the limit specified in the regulations. During bacteremia, the concentration of bacteria in blood rarely exceeds 10^3 mL^{-1} [39,40]. Other authors [15] developed a sensor for bacteria based on Magainin I immobilized on gold microelectrodes with detection limits of 10^3 CFU mL^{-1}, a clinically useful range of values. We obtained an even lower detection limit of 10^2 CFU mL^{-1} for *E. coli* and *K. pneumonia*, a result probably due to the higher affinity of ClavA to specific bacteria compared to Magainin I.

Although the R_{ct} values may vary among different electrodes because of sensor-to-sensor variability and the complexity of multiple incubation steps, the impedimetric signal was stable in the concentration range analyzed. The observed differences in the detection limits for the studied bacteria may be due to the varying degrees of the affinity of the peptide for LPS O-antigen components

Table 1
Values of the equivalent circuit elements from fitted impedance results. All electrochemical measurements were performed in triplicate using three different samples ($n = 3$).

Modified electrode	Bacteria concentration (CFU mL^{-1})	R_{CT} (kΩ)[a]	Q (μF)[a]	n[a]
Bare gold electrode	–	0.21 ± 0.02	2.20 ± 0.36	0.35 ± 0.04
ClavA-CNTs	–	10.7 ± 0.08	3.38 ± 0.41	0.77 ± 0.05
ClavA-CNTs-*E. coli*	10^2	21.1 ± 1.21	6.11 ± 1.73	1.00 ± 0.05
ClavA-CNTs-*E. coli*	10^3	32.3 ± 1.35	3.23 ± 1.46	0.95 ± 0.08
ClavA-CNTs-*E. coli*	10^4	42.4 ± 1.79	1.64 ± 0.04	0.94 ± 0.03
ClavA-CNTs-*E. coli*	10^5	47.6 ± 1.53	1.18 ± 0.09	0.81 ± 0.06
ClavA-CNTs-*E. coli*	10^6	47.5 ± 2.74	1.40 ± 0.06	0.99 ± 0.09
ClavA-CNTs-*K. pneumoniae*	10^2	25.8 ± 2.18	1.65 ± 0.04	0.48 ± 0.01
ClavA-CNTs-*K. pneumoniae*	10^3	28.6 ± 1.64	1.08 ± 0.02	0.58 ± 0.06
ClavA-CNTs-*K. pneumoniae*	10^4	30.6 ± 1.59	8.39 ± 0.07	0.62 ± 0.02
ClavA-CNTs-*K. pneumoniae*	10^5	32.9 ± 1.25	4.20 ± 0.03	0.72 ± 0.03
ClavA-CNTs-*K. pneumoniae*	10^6	37.6 ± 1.75	5.12 ± 0.05	0.68 ± 0.07
ClavA-CNTs-*E. faecalis*	10^2	16.5 ± 1.31	3.57 ± 0.47	0.73 ± 0.08
ClavA-CNTs-*E. faecalis*	10^3	17.2 ± 1.48	5.18 ± 0.39	1.00 ± 0.12
ClavA-CNTs-*E. faecalis*	10^4	18.0 ± 1.05	5.52 ± 0.89	1.00 ± 0.09
ClavA-CNTs-*E. faecalis*	10^5	21.3 ± 1.45	3.05 ± 0.68	0.78 ± 0.05
ClavA-CNTs-*E. faecalis*	10^6	22.0 ± 1.67	3.45 ± 0.34	0.76 ± 0.04
ClavA-CNTs-*B. subtilis*	10^2	11.2 ± 1.43	1.98 ± 0.05	0.84 ± 0.06
ClavA-CNTs-*B. subtilis*	10^3	13.8 ± 1.37	2.26 ± 0.06	0.64 ± 0.02
ClavA-CNTs-*B. subtilis*	10^4	14.2 ± 1.70	1.21 ± 0.05	0.95 ± 0.04
ClavA-CNTs-*B. subtilis*	10^5	14.3 ± 1.65	6.22 ± 0.19	0.64 ± 0.07
ClavA-CNTs-*B. subtilis*	10^6	16.2 ± 1.39	1.19 ± 0.06	0.98 ± 0.05

[a] Values of the equivalent circuit elements from fitted impedance results.

of the outer membranes [16,41]. In addition, other AMPs, such as cecropins, defensins, etc., may have higher affinities for one or both targets [16].

To confirm the biological recognition, we assumed that the filling of the biorecognition sites could be obtained by the bacterial surface coverage (θ) as

$$\theta = \frac{1 - R_{pep}}{R_{bact}} \quad (2)$$

where R_{pep} is the charge transfer resistance for ClavA-CNTs-Cys-modified electrode and R_{bact} is the charge transfer resistance obtained for cells unit of the bacterial cell onto ClavA-CNTs-Cys-modified electrode. In Fig. 6 we present a plot of θ as a function of concentration of bacterial CFU mL^{-1}, where one can observe that the value of θ increases with the increase in the bacterial cells concentration. At 10^4 CFU mL^{-1}, θ is found to be ~0.74 (74%) and ~0.69 (69%), for *E. coli* and *K. pneumoniae*, respectively, while lower values of θ were obtained to *E. faecalis* and *B. subtilis*.

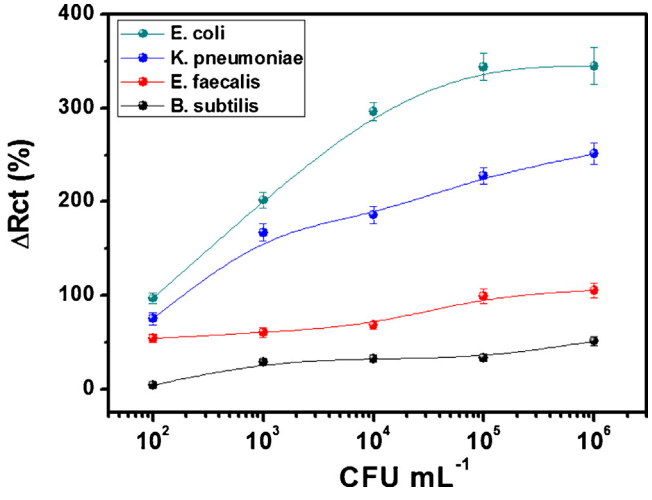

Fig. 5. ΔR_{CT}% of the sensor system after exposure to different bacterial strains. The experimental data used to calculate ΔR_{CT}% is shown in Table 1, including the standard deviation. All experiments were performed in triplicate using three different samples ($n = 3$).

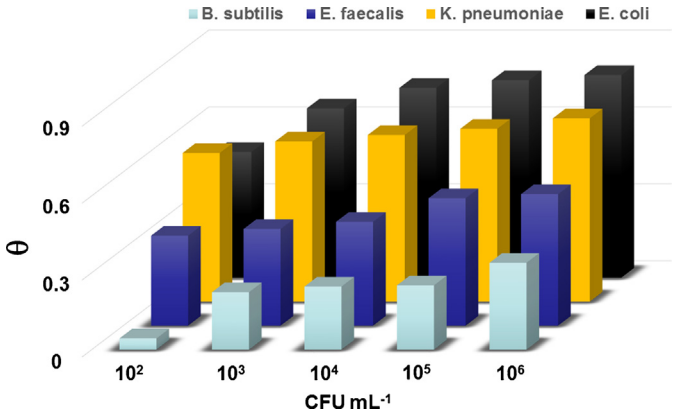

Fig. 6. Bacterial surface coverage (θ) as a function of concentration of bacterial CFU mL^{-1}. The experimental data used to calculate θ is shown in Table 1, including the standard deviation. All experiments were performed in triplicate using three different samples ($n = 3$).

4. Conclusions

We obtained a very low limit of response of the nanostructured biosensor based on CNTs and peptide in the detection of diverse bacteria at a concentration of 10^2 CFU mL^{-1}, which corresponds to ~0.1 bacterium μL^{-1}. Recently, using an interdigitated microelectrode array (IMA), Mannoor et al. [15] obtained a limit of 1 bacterium μL^{-1} (10^3 CFU mL^{-1}). The limit obtained by these authors using IMA can be attributed to the electrical double layer resulting from the electrode polarization effect at low frequencies [15]. Other authors developed immunosensors for *E. coli* with the detection limit of 10^6 CFU mL^{-1} [42] and 10^3 CFU mL^{-1} [27]. Ruan et al. [43] reported an impedimetric sensor for bacteria detection based on the use of enzyme-labeled horseradish peroxide, with a linear response between 10^4 and 10^7 CFU mL^{-1}and the detection limit of 10^3 CFU mL^{-1}. Impedimetric label-free detection of *E. coli* bacteria has also been developed [44] and the corresponding sensor showed a good performance, with a detection range of 10^3–10^7 CFU mL^{-1}.

Here, we demonstrated the development of a very sensitive nanostructured sensor that can be useful to detect the presence of infectious microorganisms belonging to a broad spectrum of

pathogenic bacteria species. A label free biosensor using carbon nanotubes and ClavA as an impedimetric platform for the detection of bacteria was obtained. From the AFM images, it can be visualized that ClavA is immobilized specifically on CNTs and that the sensor was correctly structured. An equivalent electrical circuit was effective to explain the sensing mechanism. The biosensor presented good reproducibility for $n = 3$ and low limits of detection (~0.1 bacterium μL^{-1}): for *E. coli* and *K. pneumoniae*, the lower and upper detection limits of the sensor were 10^2 CFU mL^{-1} and 10^6 CFU mL^{-1}, respectively. In the case of *E. faecalis* and *B. subtilis* the lower detection limit is 10^3 CFU mL^{-1}. The nanostructured sensor developed in this work was able to detect *K. pneumoniae*, *E. faecalis*, *E. coli* and *B. subtilis* in a specific manner, with good selectivity and sensitivity. Our sensor was able to differentiate between Gram-positive, Gram-negative, pathogenic and non-pathogenic bacteria. We demonstrated the feasibility of nanostructured systems composed by CNTs and peptide to identify microorganisms based on impedimetric measurements. Hence, the present work has introduced a simpler system for detecting and identifying pathogens when compared to traditional complex procedures.

Acknowledgements

The authors are grateful for support from the Rede de Nanobiotecnologia/CAPES, INCT_IF (Instituto Nacional de Ciência e Tecnologia para Inovação Farmacêutica), CNPq (grant 310305/2012-8 and 310361/2012-5), FAPDF and FACEPE. J.M. Nascimento would like to thank CAPES for a PhD scholarship.

References

[1] J.N. Pendleton, S.P. Gorman, B.F. Gilmore, Expert Rev. Anti Infect. Ther. 11 (2013) 297–308.
[2] R.L. Buchanan, M.P. Doyle, Food Technol. (Chicago) 51 (1997) 69–76.
[3] P.K. Mandal, A.K. Biswas, K. Choi, U.K. Pal, Am. J. Food Technol. 6 (2011) 87–102.
[4] P. Belgrader, W. Benett, D. Hadley, J. Richards, P. Stratton, R. Mariella, F. Milanovich, Science 284 (1999) 449–450.
[5] Y.G. Li, Y.T.H. Cu, D. Luo, Nat. Biotechnol. 23 (2005) 885–889.
[6] K.C. de Almeida, T.B. Lima, D.O. Motta, O. Silva, B.S. Magalhães, S.C. Dias, O.L. Franco, J. Antibiot. 67 (2014) 681–687.
[7] L. Yang, R. Bashir, Biotechnol. Adv. 26 (2008) 135–150.
[8] M.D. Lad, F. Birembaut, L.A. Clifton, R.A. Frazier, J.R.P. Webster, R.J. Green, Biophys. J. 92 (2007) 3575–3586.
[9] N.Y. Yount, M.R. Yeaman, Protein Peptide Lett. 12 (2005) 49–67.
[10] H.G. Boman, J. Intern. Med. 254 (2003) 197–215.
[11] M.R. Yeaman, N.Y. Yount, Pharmacol. Rev. 55 (2003) 27–55.
[12] I.H. Lee, C.Q. Zhao, Y. Cho, S.S.L. Harwig, E.L. Cooper, R.I. Lehrer, FEBS Lett. 400 (1997) 158–162.
[13] E.J.M. van Kan, D.N. Ganchev, M.M.E. Snel, V. Chupin, A. van der Bent, B. de Kruijff, Biochemistry 42 (2003) 11366–11372.
[14] I.H. Lee, Y. Cho, R.I. Lehrer, Infect. Immun. 65 (1997) 2898–2903.
[15] M.S. Mannoor, S.Y. Zhang, A.J. Link, M.C. McAlpine, Proc. Natl. Acad. Sci. U. S. A. 107 (2010) 19207–19212.
[16] N.V. Kulagina, M.E. Lassman, F.S. Ligler, C.R. Taitt, Anal. Chem. 77 (2005) 6504–6508.
[17] N.V. Kulagina, K.M. Shaffer, G.P. Anderson, F.S. Ligler, C.R. Taitt, Anal. Chim. Acta 575 (2006) 9–15.
[18] D. Tasis, N. Tagmatarchis, A. Bianco, M. Prato, Chem. Rev. 106 (2006) 1105–1136.
[19] W.R. Yang, P. Thordarson, J.J. Gooding, S.P. Ringer, F. Braet, Nanotechnology 18 (2007).
[20] D. Zheng, S.K. Vashist, M.M. Dykas, S. Saha, K. Al-Rubeaan, E. Lam, J.H.T. Luong, F.S. Sheu, Materials 6 (2013) 1011–1027.
[21] J. Wang, G.D. Liu, M.R. Jan, J. Am. Chem. Soc. 126 (2004) 3010–3011.
[22] J.R. MacDonald, W.B. Johnson, Fundamentals of impedance spectroscopy, in: J.R. MacDonald (Ed.), Impedance Spectroscopy – Emphasizing Solid Materials, John Wiley & Sons, New York, USA, 1987, pp. 1–26.
[23] A.M.O. Brett, C. Brett, Electrochemistry – Principles, Methods and Applications, Oxford University Press, New York, USA, 1993.
[24] Y.S. Kim, H.S. Jung, T. Matsuura, H.Y. Lee, T. Kawai, M.B. Gu, Biosens. Bioelectron. 22 (2007) 2525–2531.
[25] B. Van Dorst, J. Mehta, K. Bekaert, E. Rouah-Martin, W. De Coen, P. Dubruel, R. Blust, J. Robbens, Biosens. Bioelectron. 26 (2010) 1178–1194.
[26] L. Vazquez, L. Jaramillo, R. Lascurain, E.L. Cooper, P. Rosas, E. Zenteno, Comp. Biochem. Phys. B 113 (1996) 355–359.
[27] P. Geng, X.N. Zhang, W.W. Meng, Q.J. Wang, W. Zhang, L.T. Jin, Z. Feng, Z.R. Wu, Electrochim. Acta 53 (2008) 4663–4668.
[28] B.C. Huayhuas-Chipana, J.C.M. Gomero, M.D.P.T. Sotomayor, J. Braz. Chem. Soc. 25 (2014) 1737–1745.
[29] V. Zorbas, A. Ortiz-Acevedo, A.B. Dalton, M.M. Yoshida, G.R. Dieckmann, R.K. Draper, R.H. Baughman, M. Jose-Yacaman, I.H. Musselman, J. Am. Chem. Soc. 126 (2004) 7222–7227.
[30] M.D.L. Oliveira, C.P. de Melo, G. Oliva, C.A.S. Andrade, Colloids Surf. B 82 (2011) 365–370.
[31] O.N. Silva, I.C. Fensterseifer, E.A. Rodrigues, H.H. Holanda, N.R. Novaes, J.P. Cunha, T.M. Rezende, K.G. Magalhaes, S.E. Moreno, M.S. Jeronimo, A.L. Bocca, O.L. Franco, Antimicrob. Agents Chemother. 59 (2015) 1620–1626.
[32] O.L. Franco, FEBS Lett. 585 (2011) 995–1000.
[33] G.A. Zelada-Guillen, S.V. Bhosale, J. Riu, F.X. Rius, Anal. Chem. 82 (2010) 9254–9260.
[34] J. Strauss, A. Kadilak, C. Cronin, C.M. Mello, T.A. Camesano, Colloids Surf. B 75 (2010) 156–164.
[35] H. Hillebrandt, G. Wiegand, M. Tanaka, E. Sackmann, Langmuir 15 (1999) 8451–8459.
[36] I.O. K'Owino, O.A. Sadik, Electroanalysis 17 (2005) 2101–2113.
[37] K. Besteman, J.O. Lee, F.G.M. Wiertz, H.A. Heering, C. Dekker, Nano Lett. 3 (2003) 727–730.
[38] S. Siddiquia, Z. Dai, C.J. Stavis, H. Zeng, N. Moldovan, R.J. Hamers, J.A. Carlisle, P.U. Arumugam, Biosens. Bioelectron. 35 (2012) 284–290.
[39] J. Wain, T.S. Diep, V.A. Ho, A.M. Walsh, N.T.T. Hoa, C.M. Parry, N.J. White, J. Clin. Microbiol. 36 (1998) 1683–1687.
[40] A.S. Werner, C.G. Cobbs, D. Kaye, E.W. Hook, J. Am. Med. Assoc. 202 (1967) 199.
[41] F.R. Rana, E.A. Macias, C.M. Sultany, M.C. Modzrakowski, J. Blazyk, Biochemistry 30 (1991) 5858–5866.
[42] L.J. Yang, Y.B. Li, G.F. Erf, Anal. Chem. 76 (2004) 1107–1113.
[43] C.M. Ruan, L.J. Yang, Y.B. Li, Anal. Chem. 74 (2002) 4814–4820.
[44] M. Gamella, S. Campuzano, C. Parrado, A.J. Reviejo, J.M. Pingarron, Talanta 78 (2009) 1303–1309.